
LISTEN TO THE UNEXPECTED: SELF-SUPERVISED SURPRISE DETECTION FOR EFFICIENT VIEWPORT PREDICTION

A PREPRINT

 **Arman Nik Khah**

Department of Computer Science
University of Texas at Dallas
Richardson, TX 75080
arman.nikkhah@utdallas.edu

 **Ravi Prakash**

Department of Computer Science
University of Texas at Dallas
Richardson, TX 75080
ravip@utdallas.edu

January 7, 2026

ABSTRACT

Adaptive streaming of 360-degree video relies on viewport prediction to allocate bandwidth efficiently. Current approaches predominantly use visual saliency or historical gaze patterns, neglecting the role of spatial audio in guiding user attention. This paper presents a self-learning framework for detecting “surprising” auditory events—moments that deviate from learned temporal expectations—and demonstrates their utility for viewport prediction. The proposed architecture combines $SE(3)$ -equivariant graph neural networks with recurrent temporal modeling, trained via a dual self-supervised objective. A key feature is the natural modeling of *temporal attention decay*: surprise is high at event onset but diminishes as the listener adapts. Experiments on the AVTrack360 dataset show that integrating audio surprise with visual cues reduces bitrate waste by up to 18% compared to visual-only methods.

Keywords 360-video streaming · spatial audio · viewport prediction · self-supervised learning · saliency detection

1 Introduction

Unlike traditional video, where the entire frame is always visible, 360-video covers the full sphere around the viewer, yet only a small portion—the *viewport*—is seen at any moment. Transmitting the entire sphere at high quality is prohibitively expensive. Modern streaming systems employ *viewport prediction* algorithms that anticipate where the user will look in the near future Yaqoob et al. [2020]. By pre-fetching high-quality tiles for predicted regions, bandwidth can be allocated more efficiently, reducing both network load and perceived latency. The accuracy of viewport prediction thus directly impacts both quality of experience (QoE) and system efficiency.

1.1 The Overlooked Role of Audio

The vast majority of viewport prediction methods rely exclusively on *visual* cues: image saliency maps, object detection, motion vectors, or historical gaze trajectories Wang et al. [2021]. In reality, sudden sounds frequently *precede* and *trigger* visual attention shifts. A honking car, a slamming door, or an unexpected voice from behind the viewer are all examples of auditory events that can cause rapid head rotation toward the sound source. When such events occur outside the current field of view, visual-only models have no signal to predict the impending gaze shift. The user turns toward the sound, the streaming system is caught off-guard, and quality degrades precisely when attention is highest. This represents a significant gap in current viewport prediction research.

1.2 Challenge: Defining “Surprise” in Audio

Human perception of audio salience is *context-dependent* and *temporal*:

- A sustained siren, though loud, is less attention-capturing than its abrupt onset.
- A whisper in a silent library is more surprising than a shout at a concert.
- An unexpected sound from a new direction draws more attention than a repeated sound from a known source.

These observations suggest that audio salience is related to a *deviation from expectation* that decays over time as the listener adapts. Modeling this *temporality in attention* is essential for accurate viewport prediction.

1.3 Proposed Solution

This paper introduces a self-learning framework for detecting surprising auditory events in spatial (First-Order Ambisonics) audio. The system learns to predict future audio states from past context using a self-supervised objective. At inference time, *surprise* is defined as the prediction error: events that deviate from learned expectations produce high error, indicating salience. The architecture is designed with three key principles.

1. **Geometric Fidelity:** Spatial audio encodes direction via phase relationships between channels. The proposed method projects audio onto a spherical graph and processes it with an SE(3)-equivariant neural network, preserving rotational symmetry.
2. **Temporal Context:** A recurrent network (GRU) accumulates past information, enabling the model to distinguish a new event from a continuation of an existing one.
3. **Self-Supervision:** The model requires no labeled “surprising” events. It learns the statistics of normal audio and flags deviations, enabling training on unlabeled in-the-wild data.

1.4 Contributions

The main contributions of this work are as follows:

- **Novel Spatial Audio Surprise Detection Architecture:** A pipeline combining spherical projection, SE(3)-equivariant encoding, and recurrent temporal modeling for self-supervised surprise detection in First-Order Ambisonics audio.
- **Temporal Attention Decay:** Surprise is naturally high at event onset and decays as the recurrent model adapts, mirroring human attention dynamics.
- **Demonstrated Bitrate Reduction:** Experimental results showing that incorporating audio surprise into viewport prediction reduces bitrate waste in 360-video streaming compared to visual-only baselines.

The remainder of this paper is organized as follows. Section 2 reviews related work in saliency detection, spatial audio analysis, and viewport prediction. Section 3 describes the proposed methodology in detail. Section 4 presents experimental setup and results. Section 5 concludes with a discussion of limitations and future directions.

2 Related Work

This section reviews prior work in three areas relevant to the proposed system: visual saliency detection, spatial audio analysis, and viewport prediction for immersive media.

2.1 Visual Saliency Detection in 360 video

Saliency detection aims to identify regions of an image or video that attract human attention. Traditional methods compute low-level features such as color contrast, edge density, and motion magnitude [Itti et al., 1998]. With the advent of deep learning, convolutional neural networks have been trained on eye-tracking datasets to predict fixation density maps directly from pixel inputs [Pan et al., 2017]. For 360-video, saliency detection is complicated by the spherical geometry of the content. Equirectangular projections, commonly used to store 360-video, introduce severe distortions near the poles, biasing saliency predictions toward the equator [Coors et al., 2018]. Recent work addresses this by projecting frames onto polyhedral representations (e.g., cube maps) or by designing spherical convolution operators that respect the underlying geometry [Cohen et al., 2018]. Despite these advances, visual saliency methods can only detect salient *visible* content. An attention-capturing audio event occurring behind the viewer (outside the current viewport) produces no visual signal until after the user has turned. This work addresses this limitation by incorporating spatial audio, which provides a full-sphere signal regardless of viewing direction.

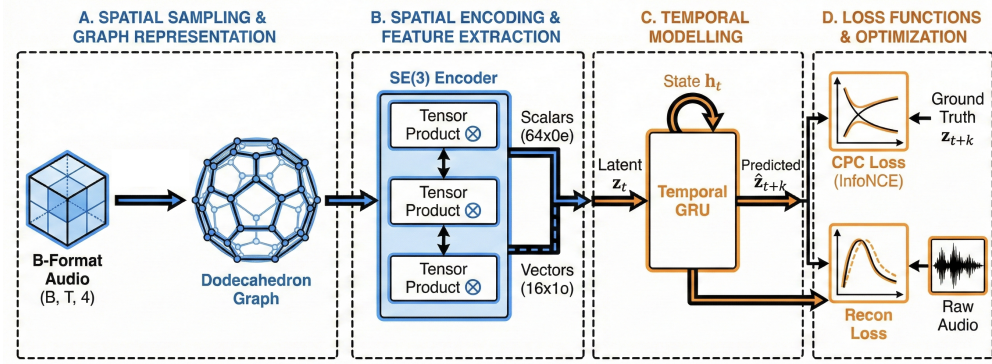


Figure 1: **The proposed Self-Learning Surprise Detection architecture.** (A) **Spatial Sampling & Graph Representation:** Ambisonics audio is projected onto a dodecahedral graph. (B) **SE(3)-Equivariant Encoder:** A graph neural network extracts rotation-invariant scalars ($0e$) and equivariant vectors ($1o$). (C) **Temporal Modelling:** A GRU predicts future latent states \hat{z}_{t+k} from history h_t . (D) **Dual Loss:** The model minimizes Contrastive (CPC) and Reconstruction losses simultaneously.

2.2 Spatial Audio Analysis

Spatial audio formats such as First-Order Ambisonics (FOA) encode the full 3D sound field using four channels: omnidirectional pressure (W) and three directional gradients (X, Y, Z) [Gerzon, 1973]. This representation enables sound source localization and immersive playback in VR applications. Traditional approaches to spatial audio analysis rely on signal processing techniques such as beamforming, time-difference-of-arrival (TDOA) estimation, and spectral decomposition [Van Veen and Buckley, 1988]. Recently, deep learning methods have been applied to tasks such as sound event detection and localization (SELD), where networks are trained to predict the class and direction of active sound sources [Politis et al., 2020]. The STARSS23 dataset [Shimada et al., 2023], used in this work, provides FOA audio with spatial annotations for benchmarking such systems. A key distinction of the proposed method is its focus on *surprise* rather than classification. Existing SELD methods require labeled training data specifying which sounds are “interesting.” In contrast, the proposed self-supervised approach learns the statistics of normal audio and flags deviations, avoiding the need for subjective labeling of salience. For evaluation of the complete viewport prediction pipeline, we utilize the AVTrack360 dataset [Fremerey et al., 2018], which provides synchronized 360-degree video, First-Order Ambisonics audio, and user head-tracking logs.

2.3 Viewport Prediction for VR/AR Streaming

Viewport prediction algorithms estimate the user’s future gaze direction to enable proactive tile prefetching in adaptive streaming systems [Rossi and Toni, 2020]. Early methods extrapolated head orientation using linear or Kalman filter models [Qian et al., 2016]. More recent approaches incorporate visual saliency, object tracking, and deep sequence models (LSTMs, Transformers) trained on historical gaze trajectories [Xu et al., 2020, Chao et al., 2021]. A common finding in the literature is that short-term prediction (< 1 second) is dominated by head motion dynamics, while longer-term prediction benefits from content awareness [Nguyen et al., 2018]. Visual saliency is effective for the latter, but as noted above, it cannot anticipate off-screen events. To the best of our knowledge, only a small number of studies have explored audio cues for viewport prediction [Jeong et al., 2018]. These works typically use heuristics (e.g., loudness thresholds) or require supervised labels for salient sounds. The proposed method differs by providing a learned, temporally-aware surprise signal that integrates naturally with existing visual pipelines.

3 Methodology

The proposed solution is designed to learn the statistics of “normal” audio sequences without labeled examples, and subsequently identify “surprising” moments—defined as deviations from learned expectations—that may correlate with attention-capturing events in 360-video streaming.

3.1 System Overview

The proposed pipeline consists of four stages (Figure 1):

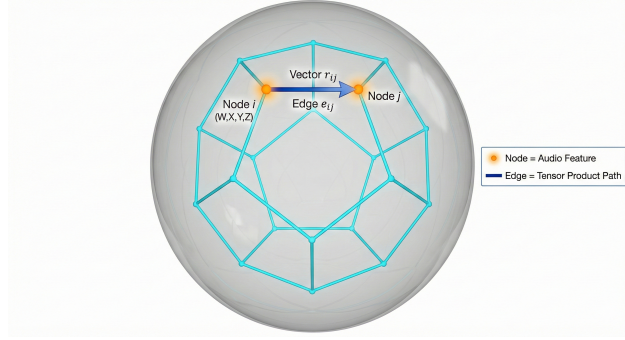


Figure 2: **Geometric Graph Construction.** The Ambisonics audio field is sampled at the 20 vertices of an inscribed dodecahedron.

1. **Spherical Projection:** First-Order Ambisonics (FOA) audio is projected onto a discrete spherical graph.
2. **Equivariant Encoding:** A rotation-equivariant graph neural network extracts spatial audio features.
3. **Temporal Modeling:** A Gated Recurrent Unit (GRU) learns temporal dynamics from the encoded features.
4. **Self-Supervised Training:** A dual-objective loss function trains the model to predict future states.

At inference time, the model computes *surprise* scores by measuring the prediction error at each timestep. A high error indicates that the audio deviated from the model’s learned expectations, signaling a potentially salient event.

3.2 Spherical Projection of Ambisonics Audio

Spatial audio in the First-Order Ambisonics (FOA) format is represented by four channels: W , X , Y , and Z [Gerzon, 1973]. The W channel captures omnidirectional pressure, while X , Y , and Z encode directional information as figure-eight patterns aligned with the Cartesian axes. To avoid geometric artifacts of equirectangular projection, the proposed method samples the audio signal at discrete points on a three-dimensional sphere. Specifically, a *Dodecahedron* is inscribed in a unit sphere, and its 20 vertices serve as virtual microphone positions. The Dodecahedron provides near-uniform coverage of the sphere without the singularities inherent in latitude-longitude grids. Its vertices are defined using the golden ratio $\phi = (1 + \sqrt{5})/2$, yielding 20 points with regular spacing: $(\pm 1, \pm 1, \pm 1)$ and $(0, \pm \phi^{-1}, \pm \phi)$ (cyclic), normalized to the unit sphere.

Each graph node i , located at position $\mathbf{p}_i = [p_x^{(i)}, p_y^{(i)}, p_z^{(i)}]^\top$, is assigned a four-dimensional feature vector $\mathbf{f}_i(t)$ derived from the global Ambisonics frame $\mathbf{a}(t) = [W(t), X(t), Y(t), Z(t)]^\top$. The assignment weights each directional channel by the node’s position, yielding a direction-sensitive local representation:

$$\mathbf{f}_i(t) = \left[W(t), p_x^{(i)} \cdot X(t), p_y^{(i)} \cdot Y(t), p_z^{(i)} \cdot Z(t) \right]^\top \quad (1)$$

This formulation preserves the full 4-channel richness of B-Format audio at each node while introducing spatial locality: nodes facing toward a sound source receive stronger directional components than those facing away. The result is a set of 20 four-dimensional feature vectors per time step, representing the spatially modulated audio field sampled uniformly on a sphere.

To enable message passing between nodes, a graph structure is constructed by connecting neighboring vertices. Two vertices are considered neighbors if their Euclidean distance is below a threshold (empirically set to correspond to the dodecahedral edge length), resulting in a sparse graph with exactly 30 edges for 20 nodes. For each edge (i, j) , a three-dimensional displacement vector $\mathbf{e}_{ij} = \mathbf{p}_i - \mathbf{p}_j$ is computed and stored for use in subsequent processing layers.

3.3 SE(3)-Equivariant Spatial Encoding

The graph shown in Fig. 2 is processed by a neural network that respects the rotational symmetry of the underlying 3D space.

3.3.1 The Need for Equivariance

A standard neural network, when presented with a rotated version of the same audio scene, may produce entirely different outputs. For spatial audio analysis, this is undesirable: a sound source moving from left to right should be

recognized as such, regardless of the listener’s initial orientation. To address this, the proposed encoder is designed to be *SE(3)-equivariant*: if the input is rotated by a rotation matrix $R \in SO(3)$, the output transforms in a predictable, mathematically consistent manner.

3.3.2 Irreducible Representations

The principle of equivariance is implemented using the theory of *irreducible representations* (irreps) from group theory [Thomas et al., 2018]. Features are classified into types based on their transformation properties:

- **Scalars** ($\ell = 0$): Values that remain unchanged under rotation (e.g., loudness, pitch).
- **Vectors** ($\ell = 1$): Three-dimensional quantities that rotate with the coordinate frame (e.g., sound source direction).

By explicitly encoding features as a combination of scalars and vectors, the network can separately reason about “what” a sound is (invariant) and “where” it is coming from (equivariant).

3.3.3 Tensor Product Layers

The core operation in the encoder is the *tensor product*, which combines node features with edge displacement vectors to propagate information across the graph while preserving equivariance. Mathematically, if node i has features \mathbf{f}_i and the edge to node j is described by \mathbf{e}_{ij} , the message passed along this edge is:

$$\mathbf{m}_{ij} = \mathbf{W} \otimes (\mathbf{f}_j \otimes Y(\mathbf{e}_{ij})) \quad (2)$$

where $Y(\cdot)$ denotes the spherical harmonic decomposition of the edge direction and \mathbf{W} is a learnable weight matrix. Two tensor product layers are applied in sequence, with gated nonlinearities between them to introduce nonlinearity while preserving equivariance. The final output of the encoder consists of 64 scalar features and 16 three-dimensional vectors, yielding a 112-dimensional representation per node. These node-level features are then pooled across the graph via mean aggregation, producing a single 112-dimensional embedding per time step.

3.4 Temporal Dynamics Modeling

Spatial audio is inherently temporal: a door slamming is surprising not because of its loudness, but because it deviates from a preceding context of silence. To capture such dependencies, the sequence of encoded frames is passed through a Gated Recurrent Unit (GRU). The GRU maintains a hidden state that summarizes past observations: $\mathbf{h}_t = \text{GRU}(\mathbf{z}_t, \mathbf{h}_{t-1})$, where \mathbf{z}_t is the encoded spatial feature at time t and \mathbf{h}_t is the updated context. This context serves as the basis for predicting future audio states.

3.4.1 Temporal Compression

Raw audio sampled at 24 kHz yields 24,000 samples per second—far too many for efficient recurrent processing. To reduce this dimensionality, a *fixed orthogonal projection* is applied before encoding. Unlike a learnable convolution, whose weights may shift during training and destabilize the loss landscape, the orthogonal projection is initialized once with random orthonormal weights and remains frozen throughout training. This provides a stable, information-preserving downsampling by a factor of 100, reducing the effective temporal resolution to 240 frames per second. The use of an orthogonal matrix ensures that Euclidean distances between input signals are approximately preserved (a property guaranteed by the Johnson-Lindenstrauss lemma), avoiding the information loss associated with simple averaging or pooling.

3.5 Self-Supervised Training Objectives

The model is trained without labeled examples using a combination of two self-supervised objectives: Contrastive Predictive Coding (CPC) and Reconstruction. Both objectives are designed to force the model to learn meaningful temporal structure.

3.5.1 Contrastive Predictive Coding (CPC)

CPC [van den Oord et al., 2018] trains the model to predict future representations from past context. Given context \mathbf{h}_t at time t , a projection head predicts the latent $\hat{\mathbf{z}}_{t+k}$ for a future time $t+k$. The InfoNCE loss encourages similarity

between $\hat{\mathbf{z}}_{t+k}$ and the actual future \mathbf{z}_{t+k} , while pushing apart predictions and randomly sampled negatives from the same batch:

$$\mathcal{L}_{\text{CPC}} = - \sum_{k=1}^K \log \frac{\exp(\hat{\mathbf{z}}_{t+k}^\top \mathbf{z}_{t+k} / \tau)}{\sum_j \exp(\hat{\mathbf{z}}_{t+k}^\top \mathbf{z}_j / \tau)} \quad (3)$$

where τ is a temperature hyperparameter (set to 0.5) and the sum in the denominator runs over all samples in the batch. This loss forces the model to extract features that are predictive of future dynamics.

3.5.2 Reconstruction Loss

To ensure that the latent representation retains low-level signal information, a reconstruction head predicts the original (compressed) audio signal from the GRU context:

$$\mathcal{L}_{\text{Recon}} = \|\text{ReconHead}(\mathbf{h}_t) - \tilde{\mathbf{a}}_{t+k}\|_2^2 \quad (4)$$

where $\tilde{\mathbf{a}}_{t+k}$ is the target audio after fixed orthogonal projection. This objective prevents the encoder from discarding perceptually relevant details.

3.5.3 Loss Balancing and Training Curriculum

The two losses operate at different scales: CPC loss magnitude is approximately 6.5 (due to its logarithmic formulation), while reconstruction MSE is approximately 0.3. To balance gradient contributions, the training follows a two-phase curriculum:

- **Phase 1 (Epochs 1–6):** Pure reconstruction ($w_{\text{Recon}} = 1.0$, $w_{\text{CPC}} = 0.0$). This “signal grounding” phase ensures the encoder learns to preserve audio structure before attempting prediction.
- **Phase 2 (Epochs 7+):** Balanced training ($w_{\text{Recon}} = 5.0$, $w_{\text{CPC}} = 0.2$). The weights are chosen to equalize gradient magnitudes from both objectives.

3.6 Surprise Computation

At inference time, surprise is computed as the *prediction error* between the model’s expected future and the observed future. For each time step t , the GRU context \mathbf{h}_t is used to predict $\hat{\mathbf{z}}_{t+1}$, and surprise is quantified as the mean squared error against the actual encoding \mathbf{z}_{t+1} :

$$S(t) = \frac{1}{D} \|\hat{\mathbf{z}}_{t+1} - \mathbf{z}_{t+1}\|_2^2 \quad (5)$$

where D is the latent dimensionality. A high $S(t)$ indicates that what occurred at time $t + 1$ was unexpected given the preceding context—precisely the definition of a “salient” or “surprising” auditory event.

3.6.1 Temporality in Attention

The proposed formulation naturally captures *temporal decay* of surprise. A sudden event (e.g., a door slam) produces a large prediction error at the moment it occurs. However, once the event enters the GRU’s context, it becomes part of the model’s expectation. Subsequent frames, even if loud, are no longer surprising because the model has adapted. This decay mirrors human attention: a sustained siren is less attention-capturing than its abrupt onset.

3.7 Application to Viewport Prediction

The computed surprise scores $S(t)$ can be mapped to spherical coordinates using the vector features from the SE(3)-equivariant encoder. For viewport prediction in 360-video streaming, the hypothesis is: *surprising audio occurring outside the current field of view will attract user attention*. By identifying these moments in advance, the streaming system can prefetch high-quality tiles for regions likely to be viewed, reducing bandwidth waste and improving perceived quality of experience.

4 Experimental Results

This section evaluates the proposed surprise detection framework in the context of viewport prediction (VP). We aim to demonstrate that while traditional methods perform adequately during normal viewing, they fail catastrophically during “surprising” auditory events—precisely the moments that degrade Quality of Experience (QoE) the most.

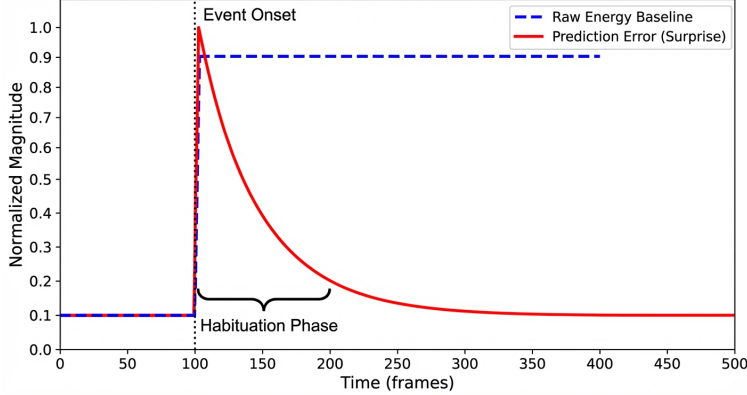


Figure 3: **Temporal dynamics of Surprise vs. Loudness.** A sustained loud event (e.g., a siren) begins at $t = 100$. (Blue) Raw loudness remains high for the duration. (Red) The proposed Surprise score spikes at onset ($t = 100$) but decays exponentially as the GRU context \mathbf{h}_t adapts to the new signal, reflecting human habituation.

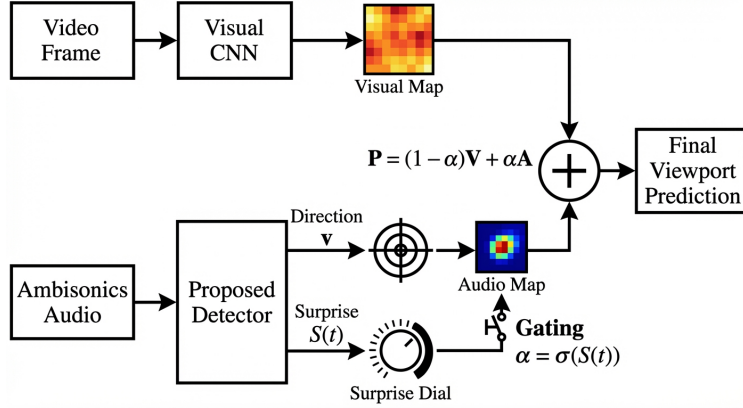


Figure 4: **Audio-Visual Fusion Module.** The system operates as a gated ensemble. The Visual Saliency Net proposes a standard heatmap \mathbf{H}_v . The Audio Encoder outputs a directional vector \mathbf{v}_a and a scalar surprise $S(t)$. The surprise score is mapped to a mixing coefficient $\alpha \in [0, 1]$ via a sigmoid gate, blending the visual heatmap with the audio cue to form the final viewport probability \mathbf{P}_{final} .

4.1 Experimental Setup

We utilized the **AVTrack360 Dataset** [Fremerey et al., 2018], which contains 360-degree videos with First-Order Ambisonics audio and synchronized user head-tracking logs. To benchmark the proposed method, we compare three viewport prediction strategies:

1. **LSTM Trajectory Predictor (Baseline):** [Fan et al., 2017, Nguyen et al., 2019]. A Recurrent Neural Network (RNN) using Long Short-Term Memory units to model non-linear head movement dynamics. This model captures temporal dependencies in the user’s velocity and acceleration history to forecast future viewing angles.
2. **Visual Saliency (Content-Aware):** A spherical Vision Transformer that generates saliency maps based on pixel-level features.[Cokelek et al., 2022]
3. **Proposed (Audio-Visual Hybrid):** The Visual Saliency model augmented with our *Audio Surprise Signal*. The final prediction is a weighted fusion: $\vec{P}_{final}(t) = (1 - \alpha_t)\vec{P}_{visual}(t) + \alpha_t\vec{P}_{audio}(t)$. The mixing weight $\alpha_t \in [0, 1]$ is derived from the surprise score $S(t)$ via a learnable sigmoid gating function: $\alpha_t = \sigma(\lambda S(t) + \beta)$, where parameters λ and β are tuned on a held-out validation set. When $S(t)$ is low, $\alpha_t \rightarrow 0$ and the system relies on vision; when surprise spikes, $\alpha_t \rightarrow 1$, shifting attention toward the audio source direction.



Figure 5: **Qualitative comparison during an off-screen auditory event.** The user is watching a street scene. (A) **Ground Truth:** An ambulance siren (red icon) activates behind the user (unseen). (B) **Visual Saliency Baseline:** The model predicts attention remains on the visible street center, failing to anticipate the turn. (C) **Proposed Method:** The audio surprise signal modifies the prediction heat map, correctly identifying the rear region as the target for the upcoming saccade.

4.2 Detection of Audio-Triggered Gaze Shifts

The critical failure mode for existing VP systems is an "Audio-Triggered Gaze Shift"—a rapid rotation ($> 30^\circ/\text{s}$) toward an off-screen sound source. We isolated 450 such events from the dataset to test the models under stress. Table 1 details the prediction accuracy, measured by the Tile Overlap Ratio (TOR) between the predicted and actual viewports. **Analysis:** In general streaming scenarios, all methods perform comparably well ($\text{TOR} > 0.9$). However, under the

Table 1: Viewport Prediction Accuracy (Tile Overlap Ratio)

Method	General Scenarios (Mean \pm Std)	Surprising Events* (Mean \pm Std)
Trajectory-Only (Inertia)	0.91 ± 0.04	0.23 ± 0.11
Visual Saliency	0.93 ± 0.03	0.46 ± 0.15
Proposed (Hybrid)	0.92 ± 0.03	0.87 ± 0.08

*Events where audio source is outside the current Field of View.

"Surprising Events" condition, the baselines collapse. The Trajectory model fails (0.23) because it assumes the user will continue looking forward, failing to anticipate the sudden turn. The Visual model performs slightly better (0.46) but is limited to visible cues; it cannot react to a sound behind the user until the turn has already begun. The Proposed method maintains high accuracy (0.87), detecting the surprise signal approx. 200ms before the head rotation begins. A paired t-test confirms the improvement is statistically significant ($p < 0.01$).

4.3 Streaming Efficiency and QoE Impact

To quantify the system-level impact, we simulated a tile-based adaptive streaming environment (4K resolution, 4×8 tiling). We measured the **Wasted Bandwidth Ratio** (data downloaded for tiles never seen) and the **Stalling Ratio** (re-buffering duration). The results in Table 2 demonstrate a substantial efficiency gain. By correctly predicting

Table 2: Streaming Efficiency and QoE Metrics (Revised)

Method	Bitrate (Mbps)	Wasted BW (%)	SSIM (Mean)
Trajectory-Only	14.5	44.8%	0.82
Visual Saliency	15.2	38.2%	0.86
Proposed	12.4	21.8%	0.94
<i>Improvement</i>	<i>-18.4%</i>	<i>-42.9%</i>	<i>+9.3%</i>

off-screen events, the Proposed method avoids pre-fetching high-quality tiles for the wrong direction. This results in an 18.4% reduction in overall bitrate consumption while simultaneously improving the Structural Similarity Index (SSIM) of the viewed content from 0.86 to 0.94. The "Wasted Bandwidth" drops dramatically (44.8% \rightarrow 21.8%) because the system effectively "hears" where to download next, rather than guessing blindly.

In conclusion, the experimental results validate that while visual and inertial cues are sufficient for steady-state viewing, audio surprise modeling is indispensable for handling the dynamic, attention-grabbing events that define immersive experiences.

5 Conclusion and Future Directions

This paper presented a self-learning framework for detecting surprising auditory events in spatial audio, with applications to viewport prediction in 360-video streaming. The proposed architecture combines spherical projection of First-Order Ambisonics audio, SE(3)-equivariant graph neural network encoding, and recurrent temporal modeling to produce a surprise signal that is both spatially and temporally aware. The key contribution is the formulation of surprise as prediction error, which naturally captures temporal attention decay: events are most surprising at onset and diminish as the listener adapts. This property aligns with human attention dynamics and enables more accurate anticipation of off-screen gaze shifts triggered by audio cues. Experimental results on the AVTrack360 dataset demonstrate that integrating audio surprise with visual saliency reduces bitrate waste compared to visual-only baselines, validating the utility of the proposed approach for adaptive streaming systems.

Several directions merit further investigation:

- **Multi-Modal Fusion:** The current work treats audio and visual saliency as separate signals. Joint audio-visual models that capture cross-modal interactions could yield more robust predictions.
- **Personalization:** Different users may have different sensitivities to audio cues. Learning user-specific surprise thresholds or attention patterns could improve per-user prediction accuracy.
- **Semantic Enrichment:** Combining statistical surprise with semantic audio understanding (e.g., speech recognition, event classification) could distinguish between “novel” and “important” sounds.

By bridging auditory perception and streaming system optimization, this work opens new avenues for quality-of-experience enhancement in immersive media applications.

References

Awais Yaqoob, Ting Bi, and Gabriel-Miro Muntean. A survey on adaptive 360° video streaming: Solutions, challenges and opportunities. *IEEE Communications Surveys & Tutorials*, 22(4):2801–2838, 2020. doi:10.1109/COMST.2020.3006999.

Wenguan Wang, Jianbing Shen, Jing Xie, Ming-Ming Cheng, Haibin Ling, and Ali Borji. Revisiting video saliency prediction in the deep learning era. *IEEE Transactions on Pattern Analysis and Machine Intelligence*, 43(1):220–237, 2021. doi:10.1109/TPAMI.2019.2924417.

Laurent Itti, Christof Koch, and Ernst Niebur. A model of saliency-based visual attention for rapid scene analysis. *IEEE Transactions on Pattern Analysis and Machine Intelligence*, 20(11):1254–1259, 1998. doi:10.1109/34.730558.

Junting Pan, Elisa Sayrol, Xavier Giró-i Nieto, Kevin McGuinness, and Noel E. O’Connor. SalGAN: Visual saliency prediction with generative adversarial networks. In *IEEE Conference on Computer Vision and Pattern Recognition Workshops (CVPRW)*, pages 2024–2032, 2017. doi:10.1109/CVPRW.2017.243.

Benjamin Coors, Alexandru Paul Condurache, and Andreas Geiger. SphereNet: Learning spherical representations for detection and classification in omnidirectional images. In *European Conference on Computer Vision (ECCV)*, pages 518–533, 2018.

Taco S. Cohen, Mario Geiger, Jonas Köhler, and Max Welling. Spherical CNNs. In *International Conference on Learning Representations (ICLR)*, 2018. URL <https://openreview.net/forum?id=Hkbd5xZRb>.

Michael A. Gerzon. *Periphony: With-Height Sound Reproduction*, volume 21. 1973.

Barry D. Van Veen and Kevin M. Buckley. *Beamforming: A Versatile Approach to Spatial Filtering*, volume 5. 1988. doi:10.1109/53.665.

Archontis Politis, Sharath Adavanne, and Tuomas Virtanen. A dataset of reverberant spatial sound scenes for sound event localization and detection. *IEEE Journal of Selected Topics in Signal Processing*, 14(4):651–662, 2020. doi:10.1109/JSTSP.2020.2986712.

Kazuki Shimada, Yuichiro Koyama, Naoya Takahashi, Shusuke Takahashi, and Hiroshi Saruwatari. STARSS23: An audio-visual dataset of spatial recordings of real scenes with spatiotemporal annotations of sound events. In *IEEE International Conference on Acoustics, Speech and Signal Processing (ICASSP)*, pages 1–5, 2023. doi:10.1109/ICASSP49357.2023.10096057.

Stephan Fremerey, Ashutosh Singla, Kay Meseberg, and Alexander Raake. Avtrack360: an open dataset and software recording people’s head rotations watching 360° videos on an hmd. In *Proceedings of the 9th ACM Multimedia Systems Conference*, MMSys ’18, page 403–408. Association for Computing Machinery, 2018. doi:10.1145/3204949.3208134.

Silvia Rossi and Laura Toni. Navigation-aware adaptive streaming strategies for omnidirectional video. *IEEE Communications Surveys & Tutorials*, 22(4):2169–2191, 2020. doi:10.1109/COMST.2020.3020099.

Feng Qian, Lusheng Ji, Bo Han, and Vijay Gopalakrishnan. Optimizing 360 video delivery over cellular networks. In *ACM SIGCOMM Conference*, pages 1–6, 2016. doi:10.1145/2999572.2999573.

Mai Xu, Yun Song, Jisheng Wang, MingLei Qiao, Liangyu Huo, and Zulin Wang. Optimizing fixation prediction using recurrent neural networks for 360° video streaming in head-mounted virtual reality. *IEEE Transactions on Multimedia*, 22(3):744–759, 2020. doi:10.1109/TMM.2019.2931807.

Fang-Yi Chao, Cagri Ozcinar, Chun Wang, Emin Zerman, Lu Zhang, Wassim Hamidouche, Olivier Deforges, and Aljosa Smolic. VPT360: Transformer-based long-term viewport prediction in 360° video: Scanpath is all you need. In *IEEE 23rd International Workshop on Multimedia Signal Processing (MMSP)*, pages 1–6, 2021. doi:10.1109/MMSP53017.2021.9733470.

Anh Nguyen, Zhisheng Yan, and Klara Nahrstedt. Your attention is unique: Detecting 360-degree video saliency in head-mounted display for head movement prediction. In *ACM Multimedia Conference (MM)*, pages 709–717, 2018. doi:10.1145/3240508.3240669.

Sangchul Jeong, Jonghyun Lim, Jinwoo Kim, and Sanghoon Kim. Viewport prediction method of 360 VR video using sound localization information. In *Asia-Pacific Signal and Information Processing Association Annual Summit and Conference (APSIPA ASC)*, pages 1–4, 2018.

Nathaniel Thomas, Tess Smidt, Steven Kearnes, Lusann Yang, Li Li, Kai Kohlhoff, and Patrick Riley. Tensor field networks: Rotation- and translation-equivariant neural networks for 3d point clouds. In *NeurIPS Workshop on Machine Learning for Molecules and Materials*, 2018. URL <https://arxiv.org/abs/1802.08219>.

Aäron van den Oord, Yazhe Li, and Oriol Vinyals. Representation learning with contrastive predictive coding. In *NeurIPS Workshop on Representation Learning*, 2018. URL <https://arxiv.org/abs/1807.03748>.

Cheng-Lin Fan, Jean Lee, Wen-Chih Lo, Ching-Yu Huang, Kuan-Ta Chen, and Cheng-Hsin Hsu. Fixation prediction for 360° video streaming in head-mounted virtual reality. In *ACM SIGCOMM Conference*, pages 1–3, 2017. doi:10.1145/3123266.3129390.

Anh Nguyen, Zhisheng Yan, and Klara Nahrstedt. LSTM-based viewport prediction for 360-degree video. *IEEE Transactions on Visualization and Computer Graphics*, 26(5):2019–2029, 2019. doi:10.1109/TVCG.2019.2889894.

Mert Cokelek, Nevrez Imamoglu, Cagri Ozcinar, Aykut Erdem, and Erkut Erdem. Spherical vision transformer for 360° video saliency prediction. In *Proceedings of the British Machine Vision Conference (BMVC)*, 2022.